Precision-cut human kidney slices as a model to elucidate the process of renal fibrosis

ELISABETH G. D. STRIBOS, THEERUT LUANGMONKONG, ANNA M. LELIVELD, IGLE J. DE JONG, WILLEM J. VAN SON, JAN-LUUK HILLEBRANDS, MARC A. SEELEN, HARRY VAN GOOR, PETER OLINGA, and HENRICUS A. M. MUTSAERS

GRONINGEN, THE NETHERLANDS; AND BANGKOK, THAILAND

Chronic kidney disease is a major health concern, and experimental models bridging the gap between animal studies and clinical research are currently lacking. Here, we evaluated precision-cut kidney slices (PCKSs) as a potential model for renal disease. PCKSs were prepared from human cortical tissue obtained from tumor nephrectomies and cultured up to 96 hours. Morphology, cell viability, and metabolic functionality (ie, uridine 5'-diphospho-glucuronosyltransferase and transporter activity) were determined to assess the integrity of PCKSs. Furthermore, inflammatory and fibrosis-related gene expressions were characterized. Finally, to validate the model, renal fibrogenesis was induced using transforming growth factor β1 (TGF-β1). Preparation of PCKSs induced an inflammatory tissue response, whereas long-term incubation (96 hours) induced fibrogenesis as shown by an increased expression of collagen type 1A1 (COL1A1) and fibronectin 1 (FN1). Importantly, PCKSs remained functional for more than 48 hours as evidenced by active glucuronidation and phenolsulfonphthalein uptake. In addition, cellular diversity appeared to be maintained, yet we observed a clear loss of nephrin messenger RNA levels suggesting that our model might not be suitable to study the role of podocytes in renal pathology. Moreover, TGF-β1 exposure augmented fibrosis, as illustrated by an increased expression of multiple fibrosis markers including COL1A1, FN1, and α-smooth muscle actin. In conclusion, PCKSs maintain their renal phenotype during culture and appear to be a promising model to investigate renal diseases, for example, renal fibrosis. Moreover, the human origin of PCKSs makes this model very suitable for translational research. (Translational Research 2016;170:8–16)

Abbreviations: ATP = adenosine triphosphate; BCRP = breast cancer resistance protein; CKD = chronic kidney disease; COL1A1 = collagen type 1A1; ECM = extracellular matrix; ESRD = end-stage renal disease; FN1 = fibronectin 1; GAPDH = glyceraldehyde 3-phosphate dehydrogenase; 7-HCG = 7-hydroxycoumarin glucuronide; HPLC = high-performance liquid chromatography; HSP47 = heat shock protein 47; LDH = lactate dehydrogenase; OAT = organic

From the Division of Nephrology, Department of Internal Medicine, University Medical Center Groningen, University of Groningen, Groningen, The Netherlands; Department of Pharmaceutical Technology and Biopharmacy, Groningen Research Institute of Pharmacy, University of Groningen, Groningen, The Netherlands; Faculty of Pharmacy, Department of Pharmacology, Mahidol University, Bangkok, Thailand; Department of Urology, University Medical Center Groningen, University of Groningen, Groningen, The Netherlands; Division of Pathology, Department of Pathology and Medical Biology, University Medical Center Groningen, University of Groningen, Groningen, The Netherlands.

Peter Olinga and Henricus A.M. Mutsaers contributed equally to this work.

Submitted for publication July 23, 2015; revision submitted November 18, 2015; accepted for publication November 20, 2015.

Reprint requests: Peter Olinga, Department of Pharmaceutical Technology and Biopharmacy, University of Groningen, Antonius Deusinglaan 1, 9713 AV Groningen, The Netherlands; e-mail: p.olinga@rug.nl.

1931-5244/$ - see front matter

http://dx.doi.org/10.1016/j.trsl.2015.11.007

anion transporter; OATP4C1 = organic anion transporting polypeptide 4C1; PAI = plasminogen activator inhibitor; PAS = Periodic acid–Schiff; PCKSs = precision-cut kidney slices; PDGFB = platelet-derived growth factor subunit B; qPCR = quantitative real-time polymerase chain reaction; TGF-β1 = transforming growth factor β1; UGT = Uridine 5′-diphospho-glucuronosyltransferase; α-SMA = α-smooth muscle actin

AT A GLANCE COMMENTARY

Stribos EGD, et al.

Background

Renal fibrosis greatly contributes to the development and perpetuation of chronic kidney disease. Currently, there are no drugs available to halt or reverse the fibrotic process, mainly because of the absence of robust experimental models for human fibrosis.

Translational Significance

Here, we provide an in-depth characterization of human precision-cut kidney slices (PCKSs), showing that the slices maintain their renal phenotype during long-term culture and that they can be used to study the early onset of renal fibrosis. More importantly, the human origin of PCKSs makes this model extremely valuable for translational research.

INTRODUCTION

Chronic kidney disease (CKD) affects approximately 10% of the adult population in developed countries.[1] CKD is irreversible and can progress to end-stage renal disease (ESRD), demanding renal replacement therapy. Yet, at this time, no effective therapy exists to halt CKD progression. Loss of functional tissue because of glomerular and tubulointerstitial accumulation of extracellular matrix proteins (ECM), that is fibrosis, is a key event in the development and perpetuation of CKD.[2] Currently, therapies for organ fibrosis in CKD patients solely focus on the origin of renal failure, for example diabetes or hypertension, and consequently have limited potential in halting fibrosis.[3,4] Therefore, insight into renal fibrogenesis might aid in the development of therapeutic approaches to prevent loss of kidney function[5] or even reverse fibrosis.

Fibrosis is a complex pathophysiological process encompassing a myriad of cells and signaling pathways. A multitude of triggers can initiate the fibrotic response, including proteinuria and glomerular immunoglobulin A deposition, yet irrespective of the initial insult, it will ultimately result in loss of organ architecture and function.[4,6] Transforming growth factor β1 (TGF-β1) is one of the key factors involved in fibrogenesis, and activation of the TGF-β1 signaling pathway will increase the expression of, among others, plasminogen activator inhibitor 1. This glycoprotein is a powerful promoter of renal fibrosis and is associated with many aggressive kidney diseases.[7] Although there is a large body of literature regarding fibrosis, the fibrotic process is still not understood completely. To elucidate the mechanisms of renal fibrosis, there is an urgent need for reliable models mimicking the human in vivo situation. Results obtained with existing animal models differ per strain,[8] and in vitro models fail to replicate the multicellular nature of the fibrotic process. Recently, Poosti et al,[9] reported the use of murine precision-cut kidney slices (PCKSs) as a suitable model to investigate renal fibrosis. PCKSs are ideal to study multicellular (pathologic) processes, for example fibrosis, because cellular diversity and organ architecture are maintained in the slices. In the present study, we aimed to improve the PCKS model by preparing slices from human tissue, and we established and characterized human PCKSs as a unique *ex vivo* model for renal disease.

MATERIALS AND METHODS

Ethics statement. This study was approved by the Medical Ethical Committee of the University Medical Centre Groningen, according to Dutch legislation and the Code of Conduct for dealing responsibly with human tissue in the context of health research (http://www.federa.org), refraining the need of written consent for "further use" of coded-anonymous human tissue. The procedures were carried out in accordance with the experimental protocols approved by the Medical Ethical Committee of the University Medical Centre Groningen.

Renal tissue. Macroscopically healthy renal cortical tissue from tumor nephrectomies was obtained and kept in ice-cold University of Wisconsin solution.

Table I. Patient demographics (n = 6)

Gender (% female)	50.0
Age (y)	55.1 ± 21.3
Nephrectomy side (% right)	100.0
Serum creatinine before nephrectomy (μmol/L)	80.2 ± 11.3
eGFR before nephrectomy (mL/min/1.73 m^2)*	77.8 ± 9.4

Abbreviation: eGFR, estimated glomerular filtration rate.
Values are presented as the mean ± standard deviation or otherwise if indicated.
*Calculated using the modification of diet in renal disease formula.

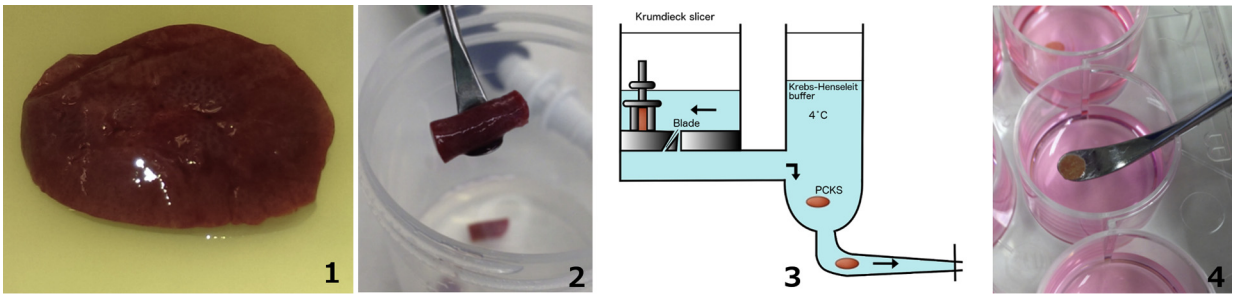

Fig 1. Workflow preparation precision-cut kidney slices (PCKSs). Cylindrical cores, 6 mm in diameter, were obtained from human renal cortical tissue using a biopsy punch (steps 1 and 2). PCKSs were prepared using the Krumdieck tissue slicer, slices with a wet weight of 4–6 mg had an estimated thickness of 250–300 μm (steps 3 and 4). Slices were subsequently incubated in optimized medium at 37°C and 80% O_2, 5% CO_2 in an incubator shaking at 90 rpm (amplitude 2 cm).

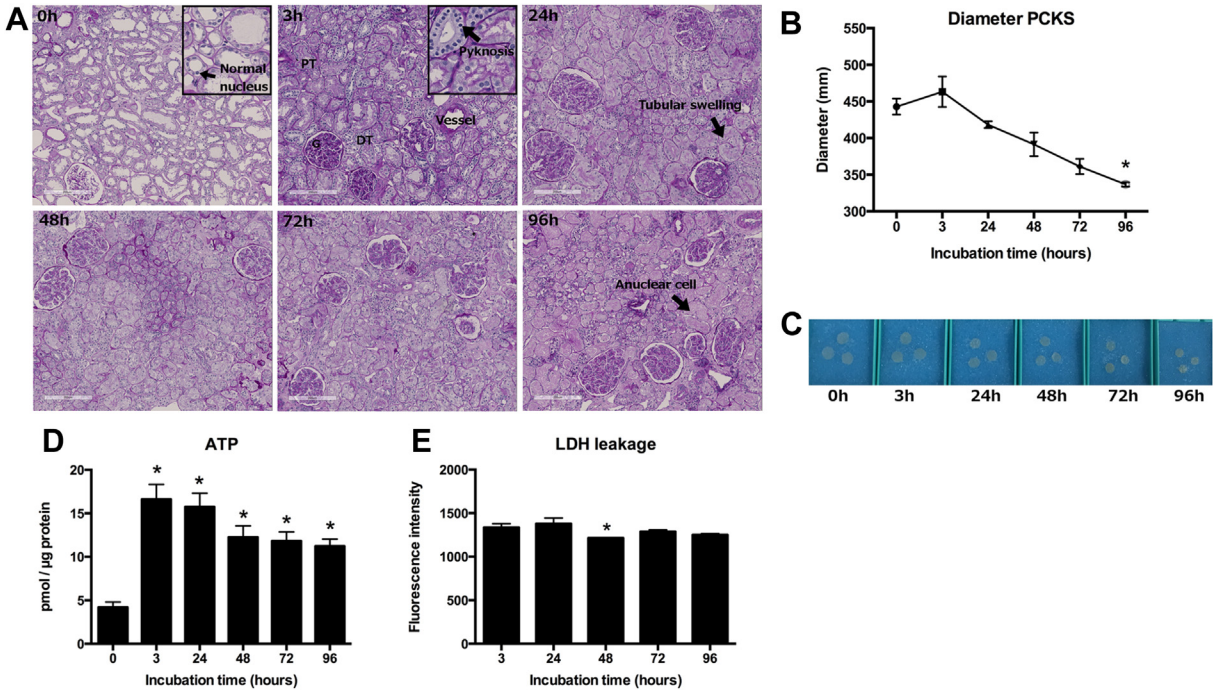

Fig 2. General morphology and viability of PCKSs. (**A**) PAS staining of PCKSs during culture, magnification, ×10; insets, magnification, ×20. (**B** and **C**) Representative figures and quantification of PCKS size during incubation, quantified using ImageJ (n = 3). (**D** and **E**) Viability of PCKSs was assessed by ATP content and LDH leakage. Data are presented as the mean ± standard error of the mean of minimally 5 independent experiments performed in triplicate. Statistical analysis was performed via a Kruskal-Wallis test followed by the Dunn multiple comparison test, compared with first column. *$P < 0.05$. PCKSs, precision-cut kidney slices.

Cold ischemia time between nephrectomy and culturing was limited to 2 hours. Patient demographics are presented in Table I.

Preparation and characterization of PCKSs. Workflow preparation of PCKSs is shown in Fig 1. In short, cylindrical cores, 6 mm in diameter, were obtained from human renal tissue using a biopsy punch. Kidney slices were subsequently prepared in ice-cold Krebs-Henseleit buffer, supplemented with 25 mM D-glucose (Merck, Darmstadt, Germany), 25 mM $NaHCO_3$ (Merck), 10 mM 4-(2-hydroxyethyl)piperazine-1-ethanesulfonic acid (MP Biomedicals, Aurora, Ohio), and saturated with carbogen (95% O_2, 5% CO_2), using a Krumdieck tissue slicer as previously described.[10] PCKSs, with a wet weight of 4–6 mg and an estimated thickness of 250–300 μm, were incubated individually in 1.3 mL of William's E medium with GlutaMAX (Life Technologies, Carlsbad) containing 10 μg/mL ciprofloxacin and 2.7 g/l D-(+)-Glucose solution (Sigma-Aldrich, Saint Louis) at 37°C in a 95% O_2, 5% CO_2 atmosphere

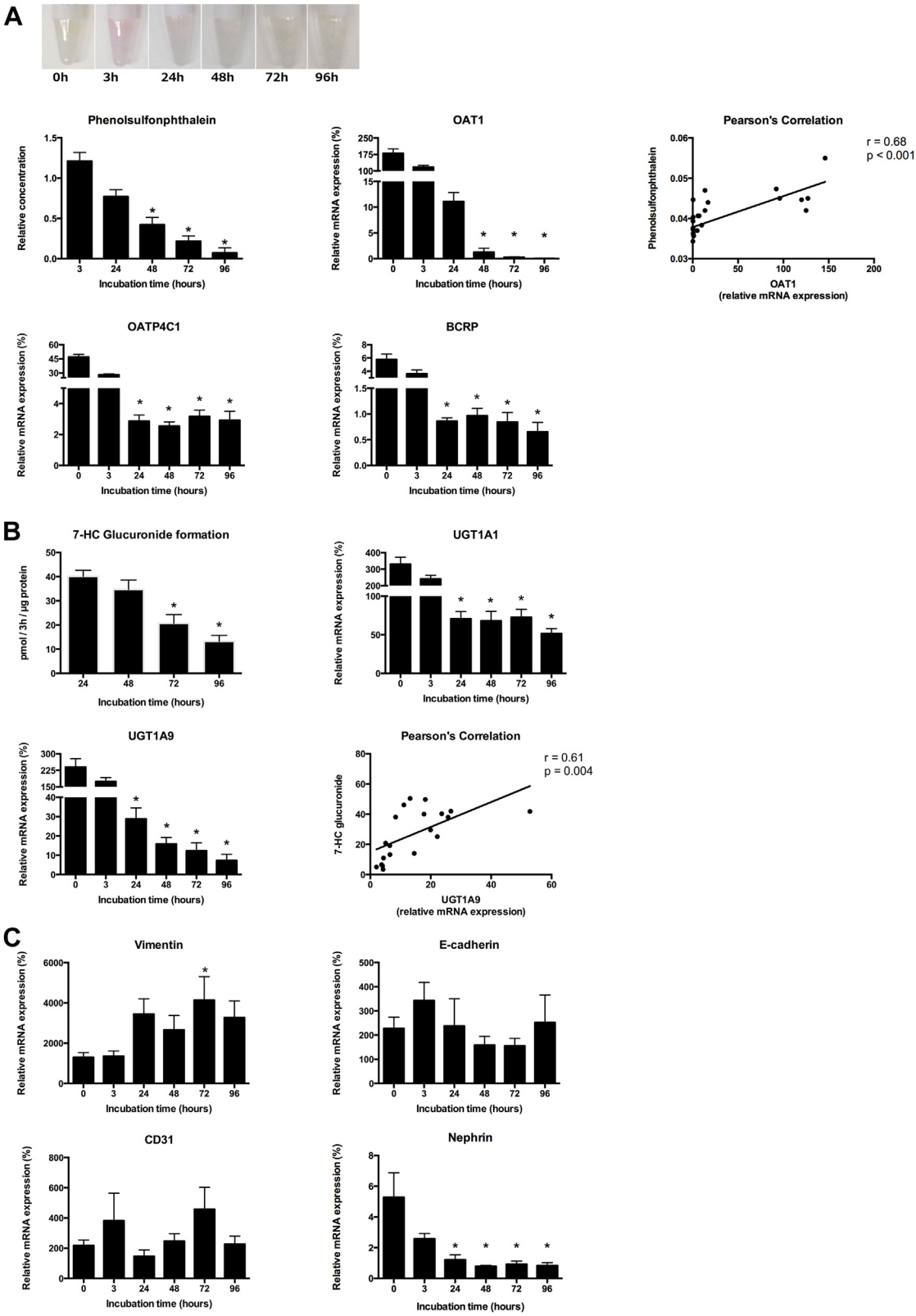

Fig 3. Functionality and cellular changes during culture of PCKSs. (**A**) Representative figures and quantification of phenolsulfonphthalein uptake in PCKSs determined by a spectrophotometer at 558 nm. (**B**) Enzyme activity was determined by HPLC. Slices were incubated with 7-HC (0.5 mM) for 3 hours at 37°C. (**A–C**) Gene expression

while gently shaken.[10] Medium was refreshed every 24 hours.

For immunohistochemistry, PCKSs were fixed in 10% formalin, embedded in paraffin, and sectioned (2 μm), and then followed by Periodic acid–Schiff (PAS) staining to assess morphology or Sirius red staining to visualize collagen protein expression. PCKS diameter was measured using ImageJ (National Institutes of Health).

Viability was determined by both adenosine triphosphate (ATP) content as previously described[11] and lactate dehydrogenase (LDH) release using the CytoTox-ONE Homogenous Membrane Integrity assay (Promega, Madison).

PCKS functionality. Uridine 5'-diphospho-glucuronosyltransferase (UGT) activity was measured by high-performance liquid chromatography (HPLC). After incubation, PCKSs were incubated with 0.5 mM 7-hydroxycoumarin for 3 hours at 37°C. Afterward, aliquots of culture medium were centrifuged (12,470 $\times$ g for 5 minutes) and injected into the HPLC system (PE-Sciex API 3000, Concord, Canada) equipped with a C18 column (150 $\times$ 2.1 mm, 5 μm; Alltech Associates, Deerfield). 7-Hydroxycoumarin metabolites were measured as previously described.[12]

To determine phenolsulfonphthalein uptake, slices were cultured as described previously and subsequently homogenized in a sonication solution containing 70% ethanol and 2 mM EDTA using a Mini-Beadbeater, and extinction of the solution was measured at 558 nm using a spectrophotometer (Synergy HT BioTek, Winooski).

Quantitative real-time polymerase chain reaction. Total RNA from untreated or exposed (5 ng/mL human TGF-β1; Roche, Basel, Switzerland) PCKSs was isolated with the RNeasy mini kit (Qiagen, Venlo, The Netherlands), using a Mini-Beadbeater for homogenization. RNA (1 μg) was reverse transcribed using the Reverse Transcription System (Promega). Subsequently, complementary DNA was used for quantitative real-time polymerase chain reaction (qPCR) performed with a 7900HT qPCR system (Applied Biosystems). Relative expression values were expressed as percentage compared with glyceraldehyde 3-phosphate dehydrogenase (GAPDH; 100%) or as fold induction using the $2^{-\Delta\Delta Ct}$ method. Used primers are listed in Supplementary Table I.

Western blot. Total protein (100 μg) was separated via sodium dodecyl sulfate–polyacrylamide gel electrophoresis using 10% gels and blotted onto polyvinylidene fluoride membranes. Antibodies used are listed in Supplementary Table II. Proteins bands were visualized using the VisiGlo Prime Horse Radish Peroxidase Chemiluminescent Substrate Kit (Amresco, Solon).

Statistics. Statistics were performed using Graphpad Prism 6.0 by either a Kruskal-Wallis test followed by the Dunn multiple comparison test or the Mann-Whitney test as appropriate. Differences between groups were considered to be statistically significant when $P < 0.05$.

RESULTS AND DISCUSSION

Characterization of PCKSs. Fig 2, *A* shows the morphology of PCKSs during incubation. As demonstrated, general morphology remains good between 3 and 72 hours with only minor signs of cellular damage (eg, pyknosis and anucleosis). Closing of tubuli was also observed probably because of a lack of preurine flow. Furthermore, PCKSs became smaller during culture (Fig 2, *B* and *C*).

Next, viability of PCKSs was assessed by ATP content and LDH leakage. ATP levels greatly increased at the start of incubation, from 4.1 (0 hours) to 16.6 pmol/μg (3 hours; Fig 2, *D*), in line with previous observations in liver slices.[13] Furthermore, ATP levels remained fairly stable during culture with a content of 11.2 pmol/μg at 96 hours. LDH levels in the culture medium were also constant (Fig 2, *E*), indicating that PCKSs remained viable. These finding are in agreement with the study from Poosti et al showing that murine PCKSs are viable up to 72 hours.[9]

Metabolic activity and cell marker expression during incubation. The kidney contributes greatly to metabolism and (transporter-mediated) solute clearance.[14] Therefore, we studied transporter activity and UGT functionality. Uptake of phenolsulfonphthalein—an organic anion transporter (OAT) substrate[15]—was observed at 3–48 hours and OAT activity time-dependently decreased with 94% between 3 and 96 hours (Fig 3, *A*), in line with the observed OAT1 gene expression ($r = 0.68$, $P < 0.001$). Furthermore, we observed mitigated expression of organic anion transporting polypeptide 4C1 and breast cancer resistance protein at the start of culture (0–24 hours), after which levels remained stable. These findings are in agreement with in vitro studies performed with primary human proximal tubular epithelial cells, in

was studied by qPCR. Relative expression was calculated using the housekeeping gene GAPDH (100%). Data are presented as the mean ± standard error of the mean of 6 independent experiments performed in triplicate. Statistical analysis was performed via a Kruskal-Wallis test followed by the Dunn multiple comparison test, compared with first column. *$P < 0.05$. BCRP, breast cancer resistance protein; 7-HC, 7-hydroxycoumarin; mRNA, messenger RNA; OAT1, organic anion transporter 1; PCKSs, precision-cut kidney slices; UGT, uridine 5'-diphospho-glucuronosyltransferase.

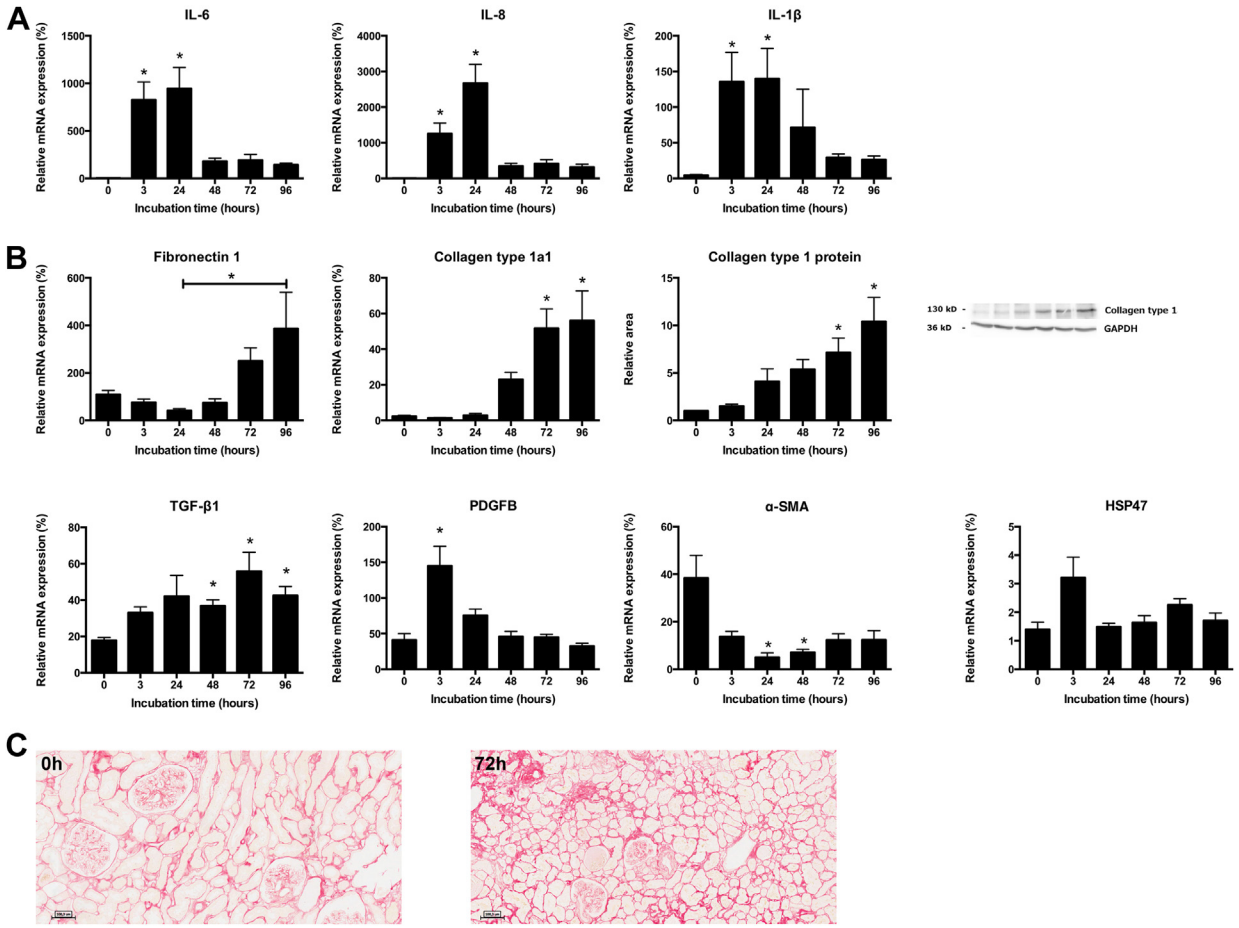

Fig 4. Expression of inflammatory and fibrosis markers during incubation of PCKSs. (**A** and **B**) Gene expression was studied by qPCR. Relative expression was calculated using the household gene GAPDH (100%). Data are presented as the mean ± standard error of the mean of 6 independent experiments performed in triplicate. Collagen type 1 protein expression was studied using Western blot (n = 3). Statistical analysis was performed via a Kruskal-Wallis test followed by the Dunn multiple comparison test, compared with 0 hours. $*P < 0.05$. (**C**) Sirius red staining of PCKSs during culture, magnification, ×20. HSP47, heat shock protein 47; IL, interleukin; mRNA, messenger RNA; PCKSs, precision-cut kidney slices; PDGFB, platelet-derived growth factor subunit B; α-SMA, α-smooth muscle actin; TGF-β1, transforming growth factor β1. For interpretation of the references to color in this figure legend, the reader is referred to the Web version of this article.

which functional expression of OATs can be sustained for a limited time.[16]

Furthermore, 7-hydroxycoumarin glucuronide formation was observed in PCKSs for more than 48 hours. Glucuronidation time-dependently decreased from 40.1 (24 hours) to 13.2 pmol/3 h/μg at 96 hours (Fig 3, *B*). Moreover, UGT activity clearly correlated with UGT1A9 gene expression ($r = 0.61$, $P = 0.004$), a main contributor to renal glucuronidation.[17] In addition, similar to organic anion transporting polypeptide 4C1 and breast cancer resistance protein, UGT1A1 expression diminished from 0 to 24 hours, after which it stayed constant. Previously, De Kanter et al[12] demonstrated UGT activity in human PCKSs during short-term (3 hours) incubation. Here, we show long-term functionality of UGTs in PCKSs, suggesting that the model is suitable for metabolism studies.

Moreover, no clear differences were observed in gene expression of vimentin, e-cadherin, and CD31 during culturing (Fig 3, *C*), suggesting that (myo)fibroblasts, epithelial cells, and endothelial cells, respectively, were not lost during incubation. Of note, although CD31 is a well-established marker for endothelial cells,[18] under pathologic conditions profibrotic renal fibroblasts can also express CD31.[19] Furthermore, we observed a marked decrease in the expression of nephrin, a podocyte marker, and key component of the slit diaphragm (Fig 3, *C*).[20] Lower nephrin levels indicate dedifferentiation or damage of podocytes, possibly induced by platelet-derived growth factor (PDGF),[21]

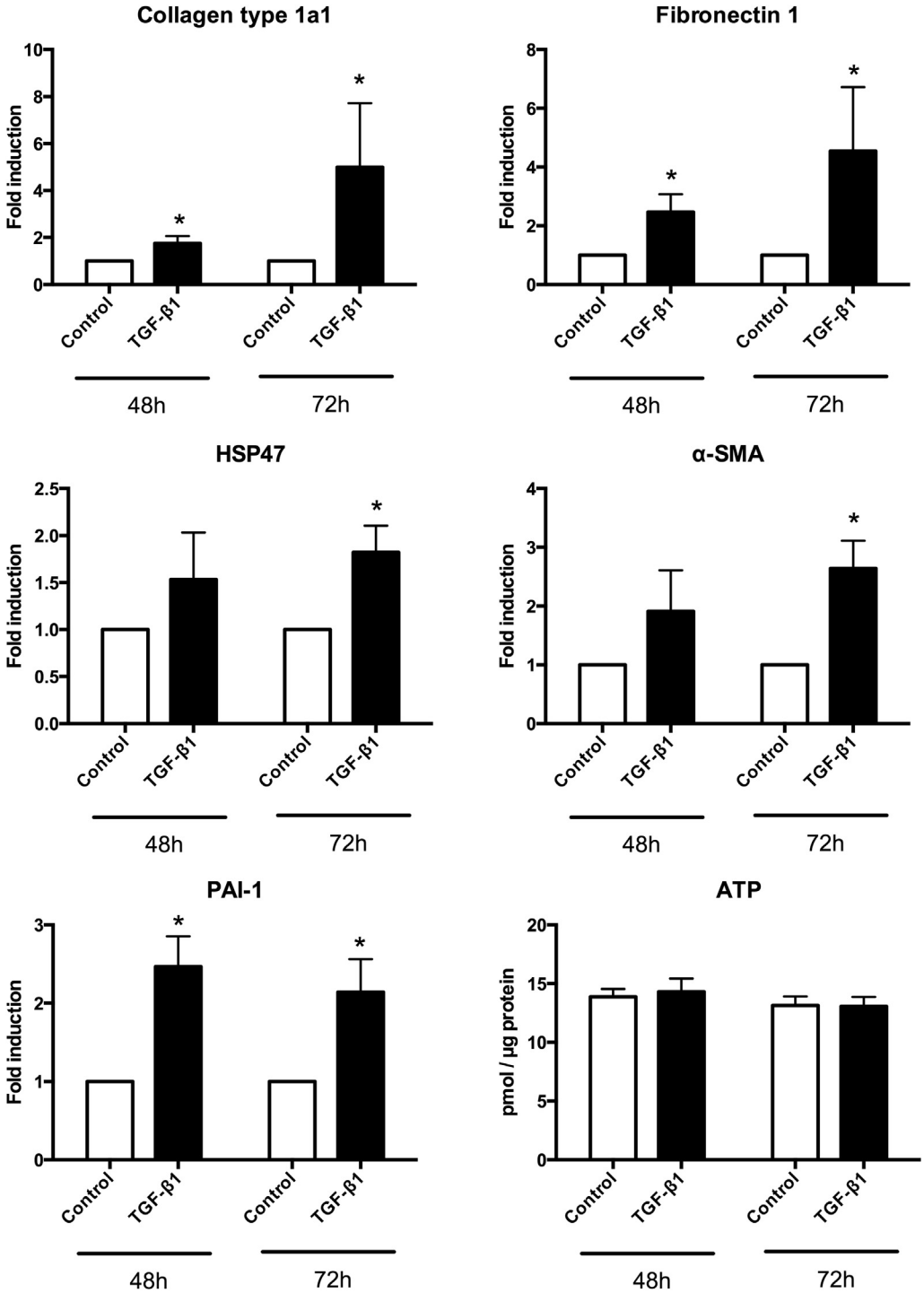

Fig 5. Induction of renal fibrosis with TGF-β1. PCKSs were treated with 5 ng/mL human TGF-β1 for either 48 or 72 hours. Subsequently, gene expression was studied by qPCR, expressed as fold induction using the $2^{-\Delta\Delta Ct}$ method, and viability was assessed by ATP content of the slices. Data are presented as the mean $\pm$ standard error of the mean of 4 independent experiments performed in triplicate. Groups were compared with control using the Mann-Whitney test. *$P < 0.05$. HSP47, heat shock protein 47; PAI-1, plasminogen activator inhibitor 1; PCKSs, precision-cut kidney slices; α-SMA, α-smooth muscle actin; TGF-β1, transforming growth factor β1.

yet is does not necessarily correlate with podocyte apoptosis.[22] Thus, the fate of podocytes in our model remains to be fully characterized.

Taken together, PCKSs behave similar to proximal tubular epithelial cells during culture, yet the major advantage of our model is that it appears to mimic and retain the cellular and architectural complexity of the kidney.

Expression of inflammatory and fibrosis markers during incubation. To assess the effect of slicing on cell stress, interleukin (IL)-6, IL-8, and IL-1β gene expressions were determined. Expressions of all 3 ILs markedly increased from 4.5% to more than 130% in the beginning of culturing (3–24 hours), after which gene expression decreased (Fig 4, *A*). These findings suggest that an early inflammatory response is evoked in PCKSs, still the trigger for the observed increase remains unclear.

With regards to fibrogenesis, we observed a marked increase in the gene expression of collagen type 1A1 (COL1A1) and fibronectin 1 (FN1) and increased type I collagen protein levels during culture (Fig 4, *B* and *C*). The observed effect was concurrent with an increased gene expression of TGF-β1. Furthermore, we detected increased gene levels of PDGF subunit B at 3 hours. Thus, the observed fibrotic response in PCKSs is likely caused by a concerted action of the TGF-β1 and PDGF pathways possibly activated by ILs. This notion is in line with previous studies showing that mechanical stress and cytokines, among other factors, drive a fibrogenic response.[23] On the contrary, gene expression of α-smooth muscle actin, a marker for matrix producing myofibroblasts,[24] first diminished from 38.4% (0 hours) to 5.0% (24 hours) and subsequently increased (12.4%; 96 hours), whereas no changes were observed in the expression of heat shock protein 47. A similar expression profile is shown in human liver slices.[13] Thus, the collagen-producing cells in PCKSs remain to be identified.

PCKSs as a model for renal fibrosis. Finally, we investigated whether the fibrotic response could be augmented in PCKSs. Therefore, we exposed PCKSs to TGF-β1, a key mediator of fibrosis.[25,26] As shown in Fig 5, treatment with TGF-β1 for 48 hours significantly increased the fibrogenic response, resulting in a more than 1.8-fold increase in gene expressions of COL1A1 and FN1, which is similar to the observations in murine PCKSs.[9] Moreover, exposure to TGF-β1 for 72 hours significantly augmented the gene levels of all the tested fibrosis markers namely COL1A1, FN1, heat shock protein 47, and α-smooth muscle actin, without affecting PCKS viability (Fig 5). Moreover, we observed an increased expression of plasminogen activator inhibitor 1, a downstream signaling molecule of the TGF-β1 pathway, indicating successful activation of the TGF-β1 signaling cascade in human PCKSs. Therefore, our model can be used to investigate renal fibrogenesis and the underlying molecular pathways.

CONCLUSIONS

We have characterized a unique ex vivo/in vitro model to investigate human renal disease, viz PCKSs. Merits of this model are the human origin of the tissue and the fact that original organ architecture is maintained. A limitation of the model is that circulating bone marrow–derived cells that contribute to the pathogenesis of fibrosis, for example macrophages,[27] are absent. In addition, the observed loss of differentiated podocytes indicates that our model is not suitable to study podocyte injury and loss as factors in renal pathology. Still, the present study with human PCKSs paves the way for a myriad of novel avenues of research including unraveling the molecular mechanism of human renal fibrosis and CKD progression and identifying potential antifibrotics. The latter might even be tested in PCKSs prepared from diseased (ie, fibrotic) instead of healthy renal tissue.

ACKNOWLEDGMENTS

Conflicts of Interest: All authors have read the journal's policy on disclosure of potential conflicts of interest and have none to declare.

This work was supported by ZonMw, grant number 114021010.

The authors thank M.M. Dekker and Suriguga for technical assistance with the morphology experiments, M.H. de Jager for performing the HPLC measurements, and J.P. Arends, MD, for his expertise in microbiology.

All authors have read the journal's authorship agreement, and the manuscript has been reviewed and approved by all named authors.

REFERENCES

1. James MT, Hemmelgarn BR, Tonelli M. Early recognition and prevention of chronic kidney disease. Lancet 2010;375:1296–309.
2. Decleves AE, Sharma K. Novel targets of antifibrotic and anti-inflammatory treatment in CKD. Nat Rev Nephrol 2014;10:257–67.
3. Lee SY, Kim SI, Choi ME. Therapeutic targets for treating fibrotic kidney diseases. Transl Res 2015;165:512–30.
4. Rockey DC, Bell PD, Hill JA. Fibrosis—a common pathway to organ injury and failure. N Engl J Med 2015;372:1138–49.
5. Cernaro V, Trifiro G, Lorenzano G, et al. New therapeutic strategies under development to halt the progression of renal failure. Expert Opin Investig Drugs 2014;23:693–709.
6. Mutsaers HAM, Stribos EGD, Glorieux G, et al. Chronic kidney disease and fibrosis: the role of uremic retention solutes. Front Med 2015;2:60.

7. Eddy AA, Fogo AB. Plasminogen activator inhibitor-1 in chronic kidney disease: evidence and mechanisms of action. J Am Soc Nephrol 2006;17:2999–3012.
8. Inoue T, Umezawa A, Takenaka T, et al. The contribution of epithelial-mesenchymal transition to renal fibrosis differs among kidney disease models. Kidney Int 2015;87:233–8.
9. Poosti F, Pham BT, Oosterhuis D, et al. Precision-cut kidney slices (PCKS) to study development of renal fibrosis and efficacy of drug targeting ex vivo. Dis Model Mech 2015;18:1227–36.
10. de Graaf IA, Olinga P, de Jager MH, et al. Preparation and incubation of precision-cut liver and intestinal slices for application in drug metabolism and toxicity studies. Nat Protoc 2010;5: 1540–51.
11. Westra IM, Oosterhuis D, Groothuis GM, et al. Precision-cut liver slices as a model for the early onset of liver fibrosis to test antifibrotic drugs. Toxicol Appl Pharmacol 2014;274:328–38.
12. De Kanter R, De Jager MH, Draaisma AL, et al. Drug-metabolizing activity of human and rat liver, lung, kidney and intestine slices. Xenobiotica 2002;32:349–62.
13. van de Bovenkamp M, Groothuis GM, Meijer DK, et al. Liver slices as a model to study fibrogenesis and test the effects of antifibrotic drugs on fibrogenic cells in human liver. Toxicol In Vitro 2008;22:771–8.
14. Mutsaers HA, Wilmer MJ, Reijnders D, et al. Uremic toxins inhibit renal metabolic capacity through interference with glucuronidation and mitochondrial respiration. Biochim Biophys Acta 2013;1832:142–50.
15. Nomura M, Motohashi H, Sekine H, et al. Developmental expression of renal organic anion transporters in rat kidney and its effect on renal secretion of phenolsulfonphthalein. Am J Physiol Renal Physiol 2012;302:F1640–9.
16. Brown CD, Sayer R, Windass AS, et al. Characterisation of human tubular cell monolayers as a model of proximal tubular xenobiotic handling. Toxicol Appl Pharmacol 2008;233:428–38.
17. Margaillan G, Rouleau M, Fallon JK, et al. Quantitative profiling of human renal UDP-glucuronosyltransferases and glucuronidation activity: a comparison of normal and tumoral kidney tissues. Drug Metab Dispos 2015;43:611–9.
18. Pusztaszeri MP, Seelentag W, Bosman FT. Immunohistochemical expression of endothelial markers CD31, CD34, von Willebrand factor, and Fli-1 in normal human tissues. J Histochem Cytochem 2006;54:385–95.
19. Zeisberg EM, Potenta SE, Sugimoto H, et al. Fibroblasts in kidney fibrosis emerge via endothelial-to-mesenchymal transition. J Am Soc Nephrol 2008;19:2282–7.
20. Herman-Edelstein M, Thomas MC, Thallas-Bonke V, et al. Dedifferentiation of immortalized human podocytes in response to transforming growth factor-beta: a model for diabetic podocytopathy. Diabetes 2011;60:1779–88.
21. van Roeyen CR, Eitner F, Boor P, et al. Induction of progressive glomerulonephritis by podocyte-specific overexpression of platelet-derived growth factor-D. Kidney Int 2011;80:1292–305.
22. Miceli I, Burt D, Tarabra E, et al. Stretch reduces nephrin expression via an angiotensin II-AT(1)-dependent mechanism in human podocytes: effect of rosiglitazone. Am J Physiol Renal Physiol 2010;298:F381–90.
23. Hinz B. The myofibroblast: paradigm for a mechanically active cell. J Biomech 2010;43:146–55.
24. Strutz F, Zeisberg M. Renal fibroblasts and myofibroblasts in chronic kidney disease. J Am Soc Nephrol 2006;17:2992–8.
25. Border WA, Noble NA. Transforming growth factor beta in tissue fibrosis. N Engl J Med 1994;331:1286–92.
26. Eddy AA. Overview of the cellular and molecular basis of kidney fibrosis. Kidney Int Suppl (2011) 2014;4:2–8.
27. Lin SL, Castano AP, Nowlin BT, et al. Bone marrow Ly6Chigh monocytes are selectively recruited to injured kidney and differentiate into functionally distinct populations. J Immunol 2009; 183:6733–43.

Appendix

SUPPLEMENTARY DATA

Supplementary Table I. Primers

Gene	Forward primer (5′–3′)	Reverse primer (5′–3′)	Taqman probe (5′–3′)
GAPDH	ACCAGGGCTGCTTTTAACTCT	GGTGCCATGGAATTTGCC	TGCCATCAATGACCCCTTCA
IL-1β	Hs01555410_m1		
IL-6	Hs00985639_m1		
IL-8	Hs00174103_m1		
COL1A1	CAATCACCTGCGTACAGA ACGCC	CGGCAGGGCTCGGGTTTC	CAGGTACCATGACCGAGACGTG
α-SMA	AGGGGGTGATGGTGGGAA	ATGATGCCATGTTCTATCGG	GGGTGACGAAGCACAGAGCA
HSP47	GCCCACCGTGGTGCCGCA	GCCAGGGCCGCCTCCAGGAG	CTCCCTCCTGCTTCTCAGCG
FN1	AGGCTTGAACCAACCTACGG ATGA	GCCTAAGCACTGGCACAACAG TTT	ATGCCGTTGGAGATGAG TGGGAA
PAI-1	CACGAGTCTTTCAGACCAAG	AGGCAAATGTCTTCTCTTCC	
TGF-β1	Hs00998133_m1		
PDGFB	Hs00966522_m1		
UGT1A1	Hs02511055_s1		
UGT1A9	Hs02516855_sH		
OATP4C1	Hs00698884_m1		
OAT1	Hs00537914_m1		
BCRP	Hs01053790_m1		
E-cadherin	Hs01023894_m1		
CD31	Hs00169777_m1		
Vimentin	Hs00185584_m1		
Nephrin	Hs00190446_m1		

Abbreviations: BCRP, breast cancer resistance protein; *COL1A1,* collagen type 1A1; *FN1,* fibronectin 1; *HSP47,* heat shock protein 47; *IL,* interleukin; *PAI-1,* plasminogen activator inhibitor 1; *PDGFB,* platelet-derived growth factor subunit B; *OAT1,* organic anion transporter 1; *OATP4C1,* organic anion transporting polypeptide 4C1; α*SMA,* α-smooth muscle actin; *TGF-β1,* transforming growth factor β1; *UGT,* UDP-glucuronosyltransferase.
All primer-probe sets were obtained from Life Technologies.

Supplementary Table II. Antibodies

Primary antibody	Secondary antibody
Rabbit-α-collagen type 1 (1:1000; Rockland Immunochemicals, Limerick)	Goat-α-rabbit (1:2000; Dako, Glostrup, Denmark)
Mouse-α-GAPDH (1:5000; Dako)	Rat-α-mouse (1:5000; Dako)